

# Research Communication

## *In Vitro* and *In Vivo* Studies Disclosed the Depigmenting Effects of Gallic Acid: A Novel Skin Lightening Agent for Hyperpigmentary Skin Diseases

K. J. Senthil Kumar<sup>1†</sup>  
M. Gokila Vani<sup>2†</sup>  
Sheng-Yang Wang<sup>3</sup>  
Jiunn-Wang Liao<sup>4</sup>  
Li-Sung Hsu<sup>5</sup>  
Hsin-Ling Yang<sup>2\*</sup>  
You-Cheng Hseu<sup>1\*</sup>

<sup>1</sup>Department of Cosmeceutics, College of Pharmacy, China Medical University, Taichung, Taiwan

<sup>2</sup>Graduate Institute of Nutrition, College of Health Care, China Medical University, Taichung, Taiwan

<sup>3</sup>Department of Forestry, College of Agriculture and Natural Resources, National Chung Hsing University, Taichung, Taiwan

<sup>4</sup>Graduate Institute of Veterinary Pathology, National Chung Hsing University, Taichung, Taiwan

<sup>5</sup>Institute of Biochemistry and Biotechnology, Chung Shan Medical University, Taichung, Taiwan

### Abstract

Gallic acid (GA) is a phenolic compound, which has been reported to suppress melanogenesis in melanoma cells. However, the molecular mechanism underlying this inhibitory effect was poorly understood. In this article, we revealed that GA down-regulated melanogenic regulatory genes including tyrosinase, tyrosinase related protein-1 (TRP-1), and dopachrome tautomerase (Dct) expression at transcriptional and translational level. In addition, GA effectively suppressed the microphthalmia-associated transcription factor (MITF) expression by down-regulating the cAMP-mediated PKA/CREB signaling cascades. To delineate the inhibition of MITF by GA, the activation of extracellular signal-regulated protein kinase (ERK) and AKT was investigated. GA caused significant increase of ERK and AKT phosphorylation, while ERK (PD98059) or AKT (LY294002) inhibitor prevents their phosphoryl-

ation and increased melanin biosynthesis. In addition, pre-treatment of MITF-siRNA significantly reduced melanin production from 100 to 40%, and even decreased into 10% by combination treatment with GA. Furthermore, UVB-induced hyperpigmentation in the mice skin was significantly rescued by topical application of GA for 4 weeks. Immunohistochemical analyses also confirmed that GA significantly inhibited melanin production followed by the down-regulation of MITF, tyrosinase and their regulatory proteins. In addition, when compared with control zebrafish, GA caused a remarkable inhibition on the endogenous pigmentation in the zebrafish. Results presented in this study strongly suggest that GA is an effective de-pigmenting or skin lightening cosmetics for topical application. © 2013 BioFactors, 39(3):259–270, 2013

**Keywords:** gallic acid; melanin; hyperpigmentation; microphthalmia-associated transcription factor; UVB-irradiation

**Abbreviations:** cAMP, cyclic adenosine monophosphate; CREB, cAMP responsible binding protein; Dct, dopachrome tautomerase; ERK, extracellular signal-regulated protein kinase; GA, gallic acid; GSK3 $\beta$ , glycogen synthase kinase 3  $\beta$ ; L-DOPA, 3,4-dihydroxyphenylalanine; MITF, microphthalmia-associated transcription factor; PKA, protein kinase A; TRP-1, tyrosinase-related protein-1; UVB, ultra violet B;  $\alpha$ -MSH,  $\alpha$ -melanocyte stimulating hormone.

© 2013 International Union of Biochemistry and Molecular Biology  
Volume 39, Number 3, May/June 2013, Pages 259–270

<sup>†</sup>K. J. Senthil Kumar and M. Gokila Vani have contributed equally.

\*Address for correspondence to: Prof. You-Cheng Hseu, Ph.D., Department of Cosmeceutics, College of Pharmacy, (or) Prof. Hsin-Ling Yang, Graduate Institute of Nutrition, China Medical University, Taichung, Taiwan. Tel.: +886-4-22053366, ext 7503; Fax: +886-4-22062891; E-mail: ychseu@mail.cmu.edu.tw (or) hlyang@mail.cmu.edu.tw.

Received 30 August 2012; accepted 6 October 2012

DOI: 10.1002/biof.1064

Published online 16 January 2013 in Wiley Online Library (wileyonlinelibrary.com)



## 1. Introduction

Pigmentation is one of the most common skin conditions affecting people of all colors and all ages worldwide. In mammals, melanin is the major pigment for the color of human skin and hair, and it is synthesized in the melanosomes of melanocytes [1]. The synthesis of both eumelanin and pheomelanin require melanocyte-specific enzymes, including tyrosinase, TRP-1, and Dct. These enzymes catalyze the conversion of tyrosine into melanin pigment [2]. Several melanin synthesis inhibitors from natural sources have been identified and utilized for cosmetic purposes, such as skin whitening or de-pigmenting agents. However, only a few agents are used as commercial skin whitening agents due to their carcinogenic potential. For example, kojic acid and arbutin were popular de-pigmenting agents before serious side effects limited their use in humans [3].

There are several signaling pathways involved in melanin biosynthesis. MITF is a basic-helix-loop (bHLH) and a leucine zipper transcription factor. MITF is known to regulate the transcription of tyrosinase, TRP-1, and Dct [4]. Moreover, the cAMP-mediated pathway is a well-known melanin synthesis cascade, and enzymatic stimulants, including  $\alpha$ -melanocyte stimulating hormone ( $\alpha$ -MSH), prostaglandin E<sub>2</sub> (PGE<sub>2</sub>), and adrenocorticotrophic hormone (ACTH) can induce the cAMP pathway. The induction of intracellular cAMP leads to protein kinase A (PKA) activation. PKA subsequently phosphorylates cAMP response-binding protein (CREB) and binds the cAMP response element (CRE) motif of the MITF promoter to activate MITF gene transcription [5]. Therefore, the use of small molecules that can trigger the signaling pathways involved in melanin biosynthesis and transformation might be useful in developing a new class of whitening or de-pigmenting agents for cosmetic purposes.

UV radiation can act directly or indirectly to induce hyperpigmentation in mammals [6]. Several reports have demonstrated phytochemicals that inhibited UVB-induced pigmentation in human or rodent skin models [7–10]. However, most screening studies tested inhibitors of melanin synthesis by directly evaluating their inhibitory potential against mushroom tyrosinase or cellular tyrosinase in melanoma or melanocytes. Melanogenesis is a complex process that involves keratinocytes and melanocytes [6]. Therefore, *in vivo* studies may provide a platform to test the efficacy of the compounds in real time.

Kim et al reported that GA inhibits melanin production in  $\alpha$ -MSH-induced B16 melanoma cells [10]. The inhibition of melanin synthesis caused by GA is mediated by the suppression of tyrosinase enzyme activity. However, the other effects of GA, including the transcription and post-translational modifications of melanogenic regulatory genes and relevant *in vivo* studies, are largely unknown. In the present study, we demonstrated that the GA-induced anti-melanogenic effect was mediated by down-regulation of melanogenic regulatory genes and their corresponding transcription factors including MITF and CREB.

## 2. Materials and Methods

### 2.1. Materials

$\alpha$ -MSH, gallic acid, kojic acid (KA), L-DOPA, dimethyl sulfoxide (DMSO), 3-[4,5-dimethyl-2-yl]-2,5-diphenyl tetrazolium bromide (MTT), and melanin were obtained from Sigma Chemical Co (St. Louis, MO). Dulbecco's modified eagle medium (DMEM), fetal bovine serum (FBS), penicillin/streptomycin, and L-glutamine were purchased from Invitrogen/Gibco Brl (Carlsbad, CA). Specific pharmacological inhibitors for ERK1/2 (PD98059) and p38 MAPK (SB203580) were obtained from Calbiochem (La Jolla, CA). All other chemicals were either reagent or HPLC grade and were supplied by either Merck (Darmstadt, Germany) or Sigma.

### 2.2. Cell Culture and Cell Viability Testing

Murine melanoma B16F10 cells were obtained from the American Type Culture Collection (ATCC, Manassas, VA) and cultured in DMEM supplemented with 10% FBS, 1% L-glutamine, and the antibiotics penicillin 100 U/mL and streptomycin 100 mg/mL unless otherwise stated. Cultured cells were maintained in a 37°C humidified incubator with 5% CO<sub>2</sub>. Cell viability was determined using a colorimetric MTT assay, as described previously by Kumar et al [11]. In brief, B16F10 cells were seeded onto a 24-well plate at a density of  $5 \times 10^4$  cells/well. After 72 h incubation with test samples or inducers, the culture medium was removed and the cells were incubated with 400  $\mu$ L of fresh DMEM containing 0.5 mg/mL of MTT for 2 h. The culture supernatant was removed and re-suspended with 400  $\mu$ L of isopropanol. The absorbance was measured at a wavelength of 470 nm using an ELISA microplate reader.

### 2.3. Determination of Melanin Content and Tyrosinase Activity

Melanin content and tyrosinase activity was determined as described previously [11]. Briefly, B16F10 cells were seeded in a 6-well plate at a density of  $2.5 \times 10^5$  cells/well. The 50% confluent cells were pretreated with GA for 2 h, and then the culture medium was replaced with fresh medium and the cells were further incubated for 24, 48, and 72 h. After incubation, the cells were harvested and washed twice with PBS, and the intercellular melanin was solubilized in 1 N NaOH. On the other hand, the melanin content was determined by measuring the absorbance at 475 nm using an ELISA microplate reader. The cultured cells were lysed using lysis buffer and clarified by centrifugation at  $11,000 \times g$  for 10 Min. Ninety microliters of each lysate containing an equal amount of protein (100  $\mu$ g) was placed into a 96-well plate, and 10  $\mu$ L of 15 mM L-DOPA or 1.5 mM L-tyrosine was added per well. After incubation at 37 °C for 20 Min, the dopachrome formation was measured at 475 nm using an ELISA microplate reader.

### 2.4. Protein Isolation and Western Blotting

B16F10 cells ( $1 \times 10^6$  cells/10 cm dish) were grown in DMEM containing 10% FBS to a nearly confluent monolayer. The cells

were incubated with GA (12.5–50  $\mu\text{M}$ ) for 2–24 H, with or without  $\alpha\text{-MSH}$ , washed with cold phosphate-buffered saline (PBS) and centrifuged at  $1500 \times g$  for 5 Min. The cell pellet was re-suspended with a mammalian protein extraction reagent (MPER) or using a nuclear and cytoplasmic extraction reagent kit (NE-PER) obtained from Pierce Biotechnology (Rockford, IL) according to the manufacturer's instructions. The fractionated-protein content was determined with Bio-Rad protein assay reagents using BSA as a standard. An equal amount of the protein fractions were subjected to 8–12% SDS-PAGE. The proteins were detected using the enhanced chemiluminescence kit (Millipore Corp., Billerica, MA), and bands were detected by ImageQuant<sup>TM</sup> LAS 4000 mini (GE Healthcare Bio-Sciences AB, Sweden).

## 2.5. Zymography Analyses

Intercellular tyrosinase activity was determined by zymography as described previously [1]. Briefly, B16F10 cells were cultured in 6-cm dish at a density of  $5 \times 10^5$  cells/dish. Then, the cells were incubated with or without GA for 48 H. The culture supernatant was collected, and the protein content in culture media was determined by Bio-Rad protein assay reagent using BSA as a standard. An equal amount of culture samples were subjected to 10% SDS-PAGE. After electrophoresis, the gels were allowed to equilibrate in 100 mM sodium phosphate buffer (pH 6.8) for 1 H and were then incubated in 30 mL of 5 mM L-DOPA until the color developed in the bands corresponding to tyrosinase. These bands appeared as dark-gray zones against a colorless background with intensity in proportion to the tyrosinase activity. The intensities of bands were visualized by ImageQuant<sup>TM</sup> LAS 4000 mini (GE Healthcare Bio-Sciences AB, Sweden).

## 2.6. RNA Extraction and RT-PCR

RNA extraction and RT-PCR were performed as described previously [12]. In brief, total RNA was extracted from cultured melanoma cells using TriZol reagent (Invitrogen). One microgram of total RNA was subjected to RT-PCR using BioRad iCycler PCR instrument (Bio-Rad, Hercules, CA) and SuperScript-III<sup>®</sup> One-Step RT-PCR platinum *taq*<sup>®</sup> Kit (Invitrogen) with appropriate PCR primers as summarized in Table 1. The PCR products were separated by 1% agarose gel, and digitally imaged after staining with ethidium bromide.

## 2.7. Immunofluorescence Assay

B16F10 cells ( $1 \times 10^4$  cells/well) were cultured in DMEM with 10% FBS in an 8-well Lab-Tek chamber (Thermo Fisher Scientific, Waltham, MA). The cells were pretreated with various concentrations of GA (12.5, 25, and 50  $\mu\text{M}$ ) for 2 h and with or without  $\alpha\text{-MSH}$  for 2 h. The cells were fixed in 2% paraformaldehyde for 15 Min and permeabilized with 0.1% Triton X-100 for 10 Min. The cells were washed and blocked with 10% FBS in PBS and then incubated for 2 H with specific primary antibody in 1.5% FBS. A FITC (488 nm) secondary antibody was incubated for another 1 H in 6% BSA. The cell nuclei were stained with a 1- $\mu\text{g}/\text{mL}$  DAPI solution for 5 Min. The stained

**TABLE 1** Primer sequences used for RT-PCR

Gene	Primer sequence	Reference
Tyrosinase	F: 5'-CAT TTT TGA TTT GAG TGT CT-3'	Lv et al. 2007
	R: 5'-TGT GGT AGT CGT CTT TGT CC-3'	
TRP-1	5'-GCT GCA GGA GCC TTC TTT CTC-3'	Lv et al. 2007
	5'-AAG ACG CTG CAC TGC TGG TCT-3'	
Dct	5'-GGA TGA CCG TGA GCA ATG GCC-3'	Lv et al. 2007
	5'-CGG TTG TGA CCA ATG GGT GCC-3'	
MITF	5'-GTA TGA ACA CGC ACT CTC TCG A-3'	Lv et al. 2007
	5'-CTT CTG CGC TCA TAC TGC TC-3'	
GAPDH	5'-ATG TAC GTA GCC ATC CAG GC-3'	Kumar et al. 2010
	5'-AGG AAG GAA GGC TGG AAG AG-3'	

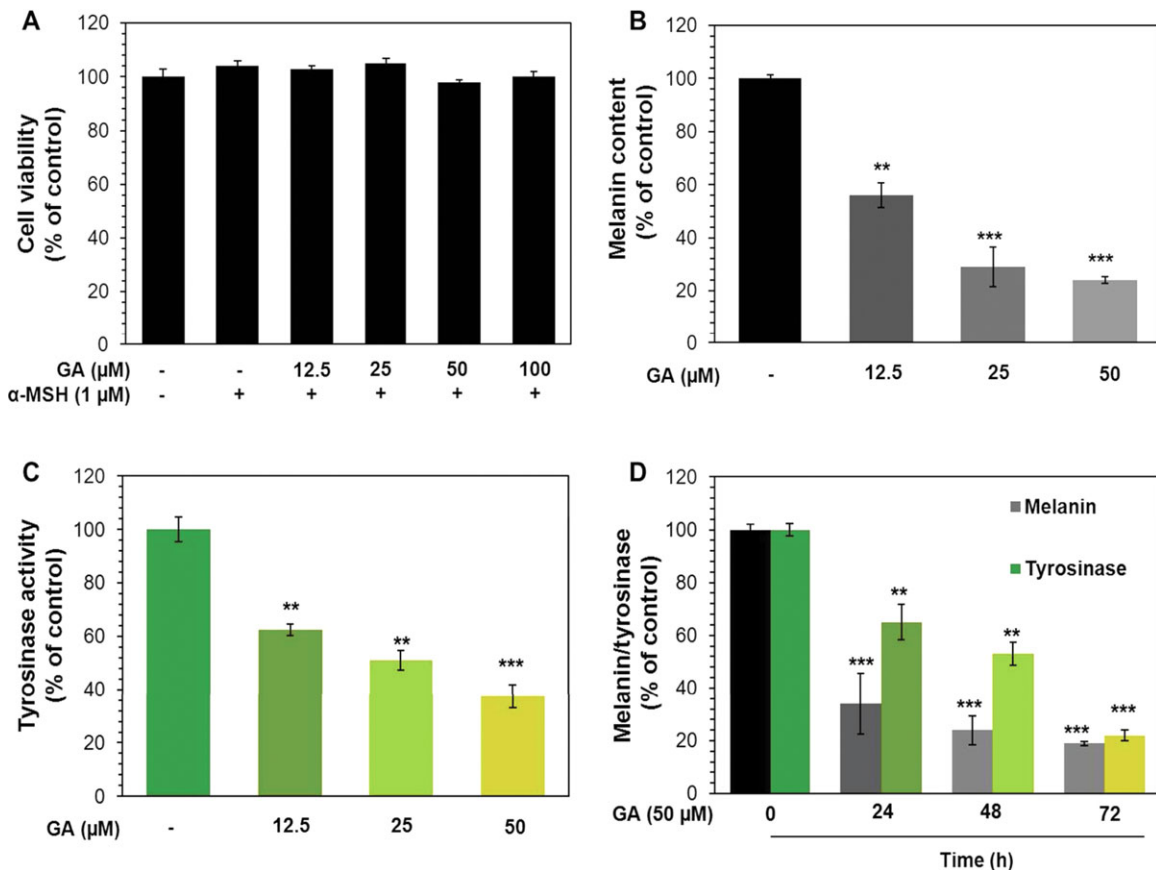
cells were washed with PBS and visualized using a fluorescence microscope at  $200\times$  magnification.

## 2.8. siRNA Transfection

siRNA was transfected with Lipofectamine RNAiMax (Invitrogen) according to the manufacturer's instructions. For transfection, B16F10 cells were plated in 6-well plates to give 40–60% confluence at the time of transfection. The next day, the culture medium was replaced with 500  $\mu\text{L}$  of Opti-MEM (GIBCOBRL/Invitrogen) and the cells were transfected using the RNAiMAX transfection reagent. In a separate tube, 100 pM of siRNA was added to 500  $\mu\text{L}$  of an Opti-MEM and RNAiMAX reagent mixture. The resulting siRNA/RNAiMAX mixture was incubated for an additional 25 Min at room temperature to allow complex formation. Subsequently, the solution was added to the cells in the 6-well plates, giving a final transfection volume of 1 mL. After 6 h incubation, the transfection medium was replaced with 2 mL of standard growth medium and the cells were cultured at 37 °C. After GA pretreatment (25  $\mu\text{M}$ ) for 2 or 48 h, the cells were then subjected to Western blot analysis or melanin quantification.

## 2.9. UVB-Induced Hyperpigmentation in C57B/6 Mice

The UVB-induced hyperpigmentation in C57B/6 (B6) was determined as described previously [13], with minor modifications. The animals were exposed to physiological UVB irradiation ( $\lambda$  max 312 nm) using  $5 \times 8\text{W}$  CL-508BL lamps (UVitec, Cambridge, UK) that were designed to allow freedom of movement during irradiation. The total UVB dose was 100  $\text{mJ}/\text{cm}^2$ /exposure. Three mice in each group were exposed to UVB thrice per week for two consecutive weeks. The whitening agents GA and KA (50  $\mu\text{M}$ ) were mixed with 1% propylene-glycol/ethanol/ $\text{H}_2\text{O}$  at a ratio of 5:3:3. This mixture was applied


**FIG 1**

The effects of GA on tyrosinase enzyme activity and melanin synthesis in melanoma cells. The cells were incubated with 0–100  $\mu\text{M}$  of GA for 48 or 72 h. (A) MTT colorimetric assay was performed to monitor the cell viability. (B) Melanin contents were quantified from total cell lysates. (C) Tyrosinase activity was measured using L-DOPA as a substrate. (D) The time-dependent inhibition of melanin production and tyrosinase activity was quantified. The results are presented as the mean  $\pm$  SD of three independent experiments. Statistical significance \* $P < 0.05$ , \*\* $P < 0.01$ , and \*\*\* $P < 0.001$  were defined as control versus sample.

topically (10  $\mu\text{L}/\text{ear}$ ) to the hyperpigmented ears once a day for 4 weeks. The skin color was evaluated by chromametry (Chromameter, CR-200, Minolta, Japan). A protocol for quantification of the  $\Delta L$ -value, a parameter for skin lightening, was adopted from Kim et al [10]. The hyperpigmentation of the ear region was photographed at each time point. After 4 weeks, the animals were anesthetized with diethyl ether and killed prior to ear sampling. The ear sections were immediately placed in 10% neutral buffered formalin for further experiments.

### 2.10. Immunohistochemical Staining

Biopsied skin tissues were embedded in paraffin and cut into 3-mm-thick sections. To study the cutaneous expression of pigment markers, the tissue sections were stained and analyzed using a light microscope. The slides were either stained by hematoxylin and eosin (H&E) or immunohistochemically stained with a rabbit polyclonal anti-tyrosinase antibody, a mouse monoclonal MITF antibody, or a rat polyclonal anti-L-DOPA antibody for 2 h at room temperature. The secondary detection antibody was conju-

gated to a DakoCytomation REAL<sup>TM</sup> EnVision<sup>TM</sup> Detection System (DakoCytomation A/S, Denmark).

### 2.11. Statistical Analyses

The results are presented as the mean  $\pm$  standard deviation (mean  $\pm$  SD). All study data were analyzed using analysis of variance, followed by Dunnett's test for pair-wise comparisons. The statistical significance was defined as \* $P < 0.05$ , \*\* $P < 0.01$ , and \*\*\* $P < 0.001$  for all tests.

## 3. Results

### 3.1. Inhibitory Effects of GA on Melanin Production and Tyrosinase Activity in Melanoma Cells

Utilizing *in vitro* studies, the effects of GA on cell viability were assessed by MTT colorimetric assay. As shown in Fig. 1A, GA had no cytotoxic effects on B16F10 melanoma cells at concentrations ranging from 12.5 to 100  $\mu\text{M}$  for 72 h, whereas GA treatment significantly and dose-dependently inhibited the cellular melanin content in melanoma cells (Fig. 1B). The inhibitory concentration leading to 50% inhibition ( $\text{IC}_{50}$ ) of melanin

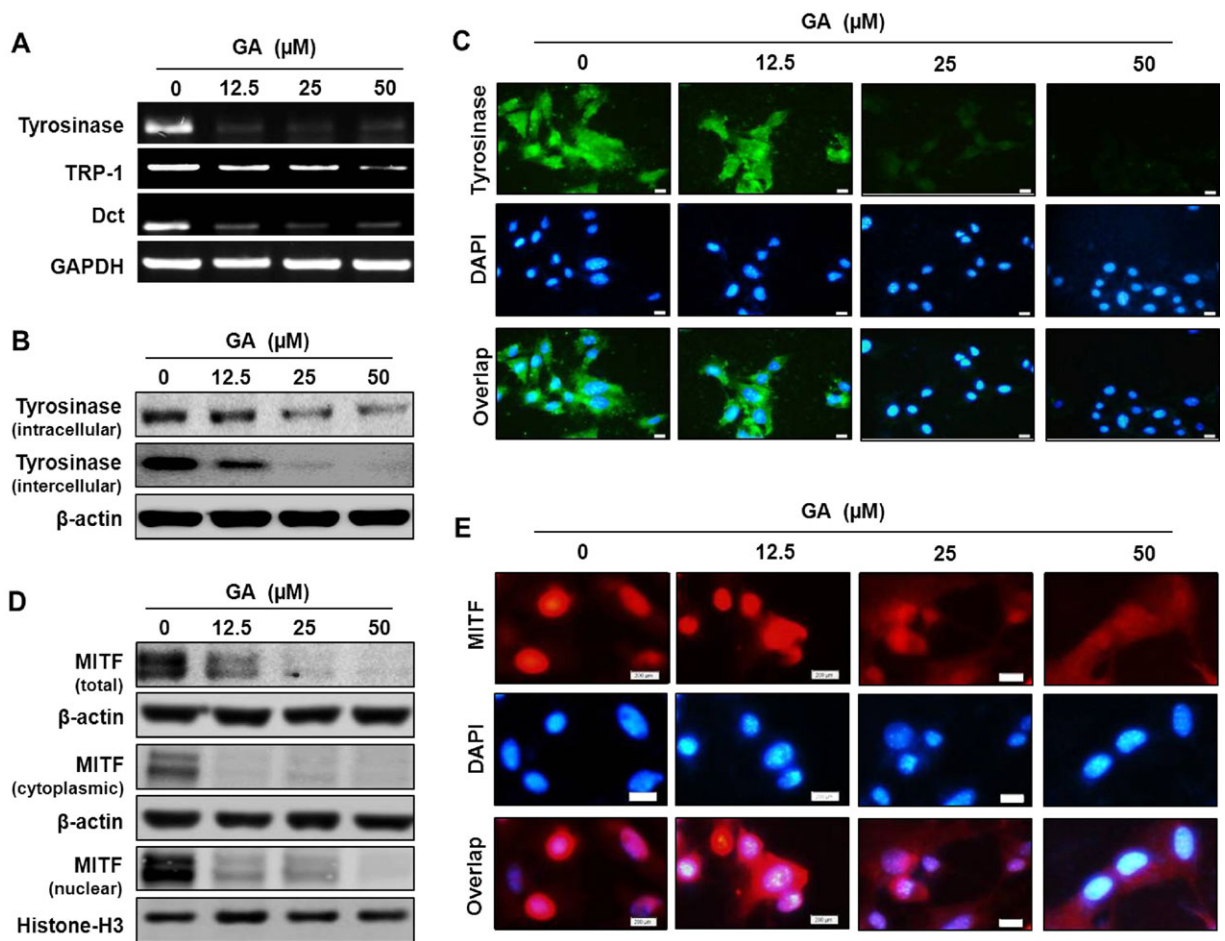


**FIG 2**

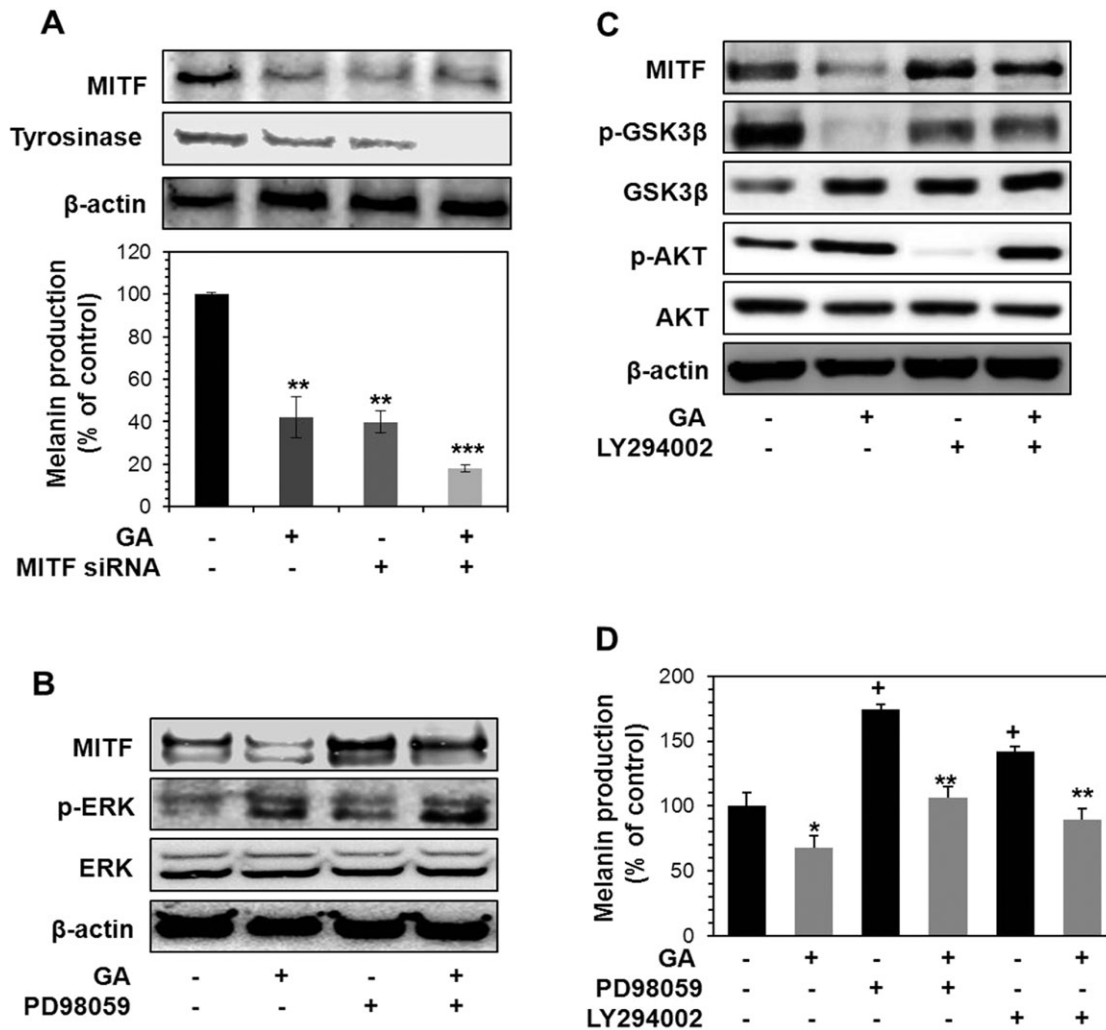
GA inhibits melanogenic regulatory protein expression in melanoma cells. (A) The tyrosinase, TRP-1, and Dct mRNA levels in GA-treated cells were semi-quantified by RT-PCR analyses. (B) Western blotting and zymography were used to quantify the intra- and intercellular tyrosinase expression in melanoma cells. (C) Tyrosinase protein expression was monitored using immunofluorescence assay. (D) MITF expression in cytoplasm and nucleus were monitored using specific cytoplasmic and nuclear extracts. (E) Immunofluorescence analyses were used to visualize the intracellular accumulation MITF in melanoma cells. The results are presented as the mean  $\pm$  SD of three independent experiments.

production was estimated to be 18.3  $\mu\text{M}$ . Furthermore, tyrosinase activity was significantly inhibited by GA with an IC<sub>50</sub> value of 24.8  $\mu\text{M}$  (Fig. 1C). In addition, these effects were also observed in a time-dependent manner (Fig. 1D).

### 3.2. GA Down-Regulates the Expression of Melanogenesis Regulatory Genes

GA-induced inhibition of melanin production was further examined by measuring the expression of melanogenic regulatory genes, including tyrosinase, TRP-1, and Dct, at the transcriptional and post-translational levels. As shown in Figs. 2A and 2B, GA significantly and dose-dependently down-regulated the expression of tyrosinase, TRP-1, and Dct at both the mRNA and protein levels. The GA-induced inhibition of tyrosinase was significantly higher than that of TRP-1 or Dct (Fig. 2A). Further analysis by immunofluorescence confirmed that the expression of tyrosinase was significantly inhibited by GA in a

dose-dependent manner (Fig. 2C). A time-dependent reduction in the protein levels of tyrosinase was also observed in response to GA treatment (data not shown). In addition, zymography analysis with L-DOPA provided positive evidence that the intercellular levels of tyrosinase enzyme were significantly reduced by GA (Fig. 2B, middle panel). This result demonstrates that GA treatment can modulate the cellular machinery to regulate melanogenesis in addition to its anti-oxidative potential for reducing the oxidation of L-tyrosine or L-DOPA [14]. Tyrosinase and its related genes are known to be transcribed by MITF [15]. Therefore, we examined whether GA could modulate the expression and nuclear translocation of MITF using Western blot and immunofluorescence assays. As shown in Fig. 2D, the endogenous MITF expression was significantly decreased by GA in a dose-dependent manner. In addition, Western blotting with the nuclear protein fraction revealed that GA not only inhibited the expression of MITF but


**FIG 3**

The effects of different inhibitors on melanin synthesis in melanoma cells. (A) The MITF gene was knocked-down by MITF siRNA. The melanin contents and protein levels of MITF and tyrosinase were measured by ELISA and Western blotting, respectively. (B,C) Melanoma cells were incubated with ERK inhibitor PD98059 or AKT inhibitor LY294002 with or without GA for 1 H and then cultured for 2 H. Western blotting was performed to monitor the MITF expression and phosphorylation of ERK, AKT, and GSK3 $\beta$ . (D) Melanin content was measured using ELISA. The results are presented as the mean  $\pm$  SD of three independent experiments. Statistical significance \* $P < 0.05$ , \*\* $P < 0.01$ , and \*\*\* $P < 0.001$  were defined as control versus sample.

also suppressed its nuclear translocation (Fig. 2D). An immunofluorescence assay also confirmed when compared with control cells, MITF expression in the nucleus was decreased by GA in a dose-dependent manner (Fig. 2E). These results suggest that the anti-melanogenic effect of GA is associated with the down-regulation of the MITF signaling pathway.

### 3.3. MITF Knockdown Inhibits Tyrosinase Expression and Reduces Melanin Production in B16F10 Cells

To further elucidate the role of MITF in GA-induced inhibition of melanogenesis, B16F10 cells were transfected with MITF siRNA (100 pM) for 6 h. The cells were then incubated with GA (25  $\mu$ M) for 2–48 H. The transfection of MITF siRNA significantly decreased the expression of MITF and its transcriptional target

tyrosinase (Fig. 3A). However, the pronounced inhibition of MITF and tyrosinase was also observed when cells were co-treated with GA for 2 H (Fig. 3A). Concomitantly, the transfection with MITF siRNA significantly decreased melanin production to  $39 \pm 6\%$  that of controls. Melanin production further declined to  $18 \pm 2\%$  when cells were co-treated with GA for 48 H. These data confirmed that GA potentially down-regulates MITF expression in B16F10 melanoma cells.

### 3.4. GA-Induced Down-Regulation of MITF is Mediated by Activation of the ERK Pathway

Previous studies have demonstrated that activation of ERK by steel factors could degrade MITF following phosphorylation at serine residues -73 and -409 [16]. Therefore, we examined whether GA could modulate the ERK pathway. As shown in

Fig. 3B, GA (25  $\mu$ M) was shown to augment ERK phosphorylation, and this effect caused MITF degradation. To clarify this effect, we examined whether PD98059, a specific ERK inhibitor, could rescue GA-induced MITF degradation and melanin synthesis. The results indicate that PD98059 increased MITF expression and melanin synthesis following the inhibition of ERK activation in melanoma cells (Figs. 3B and 3D). However, a co-treatment with GA significantly prevented PD98059-induced MITF expression and melanin synthesis by increasing ERK phosphorylation (Figs. 3B and 3D). These results suggest that the GA-induced anti-melanogenic effect may be mediated by activation of the ERK pathway.

### 3.5. The AKT/GSK3 $\beta$ Signaling Pathways are Involved in the GA-Induced Down-Regulation of MITF

Because the activation of AKT/GSK3 $\beta$  decreases melanin synthesis [16], we examined whether GA could regulate AKT/GSK3 $\beta$  activation in melanoma cells. As shown in Fig. 3C, GA caused a significant increase in the phosphorylation of AKT/GSK3 $\beta$  and decreased MITF expression. To confirm this mechanism, we used LY294002, a pharmacological inhibitor of AKT, to assess the role of AKT/GSK3 $\beta$  in GA-induced inhibition of MITF. As we expected, MITF expression and melanin synthesis were significantly augmented after treatment with LY294002. Furthermore, co-treatment with GA considerably prevented the LY294002-induced MITF expression and melanin synthesis by restoring AKT/GSK3 $\beta$  phosphorylation (Figs. 3C and 3D). These results indicate that treatment with GA also down-regulates melanin production through the activation of the AKT/GSK3 $\beta$  signaling pathway.

### 3.6. The GA-Induced Down-Regulation of MITF is Mediated by the PKA/CREB Signaling Pathway

We hypothesized that GA could modulate MITF expression at the transcriptional level. RT-PCR analysis revealed that GA caused a significant reduction in MITF expression at the transcriptional level (Fig. 4A). After the stimulatory binding of  $\alpha$ -MSH to MC1-R, adenylyl cyclase is activated and cAMP is produced. The production of cAMP induces the PKA pathway to activate the CREB transcription factor. CREB, which mediates MITF promoter activation to induce melanin production [17]. Therefore, we sought to monitor the effect of GA on  $\alpha$ -MSH-induced activation of CREB and their nuclear translocation by Western blot and immunofluorescence assays. Compared with control cells, GA treatment significantly suppressed the phosphorylation of CREB, whereas no significant change was observed in total CREB levels (Fig. 4B). Similarly, GA caused a reduction in the phosphorylation of PKA, followed by the suppression of cAMP and MCR-1 in a dose-dependent manner (Fig. 4B). An immunofluorescence assay confirmed that GA significantly prevents the nuclear translocation of CREB. Our results also indicate that the phos-CREB protein was predominantly located in the cytoplasmic region (Fig. 4C). These data suggest that GA reduces the phosphorylation of CREB, which

leads to the subsequent reduction of MITF transcription and inhibits melanin production.

### 3.7. The Effects of GA on Endogenous Body Pigmentation in Zebrafish

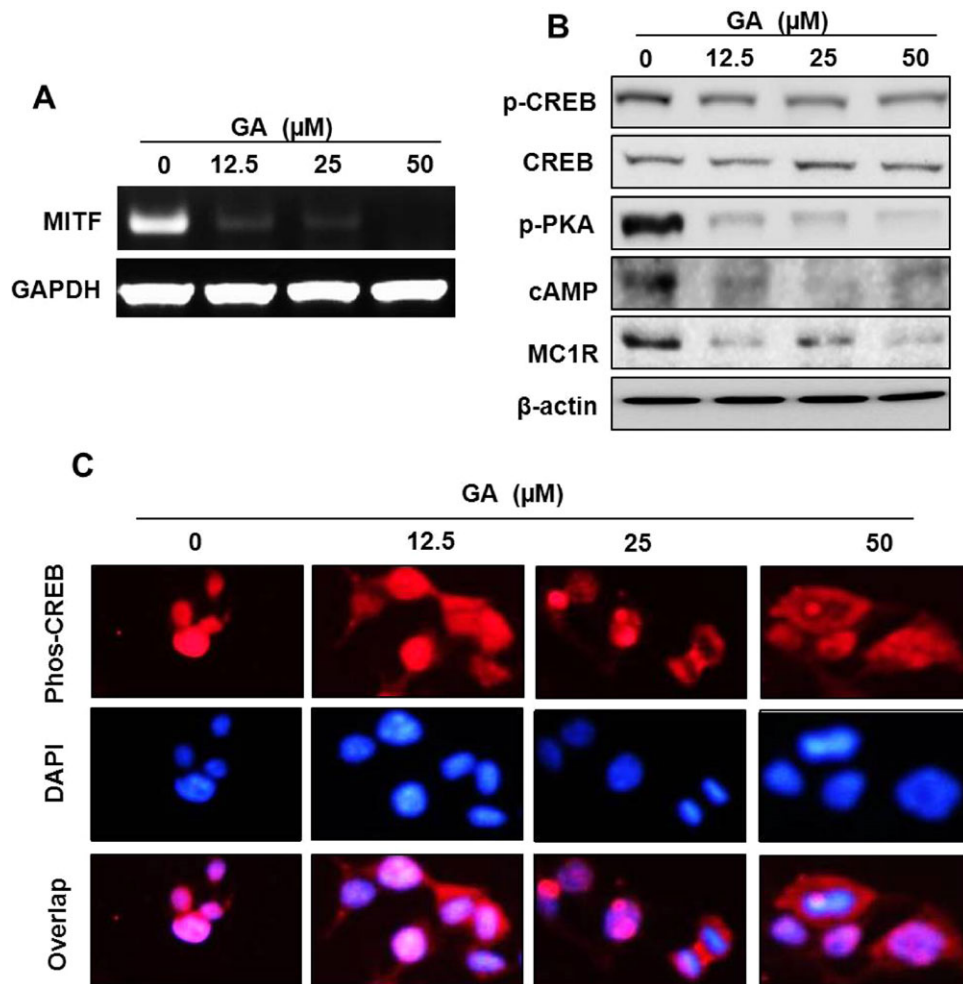
A phenotype-based evaluation of skin whitening agents provides reliable data for further experimentation [10]. It is known that zebrafish have melanin pigmentation on their body surface. This feature allows simple observations of the pigmentation processes without complicated experiments. As shown in Fig. 5A, the body pigmentation in the zebrafish was remarkably decreased when 24 h post-fertilized embryos were exposed to GA for 36 h. A quantitative analysis showed that GA treatment decreased the body pigmentation by  $56 \pm 11$  and  $41 \pm 6\%$  at GA concentrations of 25 and 50  $\mu$ M, respectively (Fig. 5A). However, when embryos were exposed to GA, no lethal effects were observed. Moreover, a comparison of body pigmentation in GA treated and control zebrafish directly indicates that the dramatic reduction in dark pigmentation by GA may be due to the decrease in proliferation and/or differentiation of melanocytes.

### 3.8. GA Abrogates UVB-Induced Hyperpigmentation in C57B/6 Mouse Ear Skin

The *in vivo* de-pigmenting effect of GA was examined using a UVB-induced hyperpigmentation model in the ear skin of B6 mice. The ear skin of B6 mice is an excellent UV-induced pigmentation model because, unlike trunk/fur-bearing skin, the epidermis of the ear contains a vast number of melanocytes [13]. GA and KA were topically applied to the UVB-induced, hyper-pigmented ear skin of B6 mice twice a day for 4 consecutive weeks. KA, a well-known skin whitening agent, was used as a positive control because it is known to prevent melanin synthesis in the skin [18]. As shown in Fig. 5B, a visible tanning of ear skin was observed after 2 weeks of UVB exposure. A substantial decrease in hyperpigmentation was observed after 4 weeks of GA treatment. The whitening effect of GA is comparable to that of KA. A quantitative evaluation of whitening was performed to rate skin lightening ( $\Delta L$ -value) before GA treatment and within 2 and 4 weeks of GA treatment. Figure 5C shows that a decrease in UVB-induced hyperpigmentation was observed at 4 weeks after the treatment with GA ( $\Delta L = 5.8 \pm 1.3$ ) when compared with the vehicle control group ( $\Delta L = 1.7 \pm 1.3$ ).

### 3.9. UVB-Induced Inflammation is Recovered by GA

Histological analyses were performed on the hyper-pigmented and GA-treated ear skin tissues of B6 mice. The H&E staining was nonspecific and was not intended to identify melanin or melanocytes; instead, it was used to observe the cellular morphology and the possible signs of inflammation. Mouse ear skin was irradiated with UVB (100 mJ/cm<sup>2</sup>) twice a week for 2 weeks. This irradiation caused a slight inflammation in the skin, as directly measured by the inflammatory markers: skin thickening and inflammatory cell infiltration. The UVB-induced


**FIG 4**

GA-induced inhibition of MITF is mediated by PKA/CREB signaling pathway. (A) The MITF mRNA level in GA-treated cells was semi-quantified by RT-PCR analyses. GAPDH was used as a loading control. (B) GA inhibits the cAMP pathway in  $\alpha$ -MSH-induced melanoma cells. Melanoma cells were pre-incubated with  $1 \mu\text{M}$  of  $\alpha$ -MSH for 1 H and then treated with GA for 2 H. Whole-cell lysates were subjected to Western blotting with specific antibodies. (C) Immunofluorescence analyses of the intracellular accumulation phos-CREB. The results are presented as the mean  $\pm$  SD of three independent experiments.

skin thickening was increased from  $23.8 \pm 4.5$ -pixel to  $14.03 \pm 1.36$ -pixel (control). The UVB-induced skin thickening and inflammatory cell infiltration was significantly decreased to  $16.3 \pm 1.12$ -pixels by the topical application of GA (Fig. 6A).

### 3.10. GA Down-Regulates Melanocyte Activation in UVB-Irradiated B6 Mouse Skin

The positive identification of pigmented melanocytes was confirmed by immunohistochemical analyses with monoclonal anti-L-DOPA and anti-melanoma Gp100 antibodies. The images of the skin sections obtained by L-DOPA staining shows spotted DOPA-positive areas (see arrow in Fig. 6B) in both control and UVB-irradiated groups. However, DOPA-positive melanocytes were barely observed in the GA treatment groups. UVB irradiation caused a very significant increase of DOPA-positive melanocytes (1.52-fold), whereas GA treatment significantly reduced DOPA-

positive cells to 0.20-fold. The immunohistochemical staining of melanosomes showed that UVB treatment caused a 3.5-fold increase, whereas GA treatment markedly inhibits (1.6-fold) the UVB-induced melanosome activation in B6 mouse skin (Fig. 6C).

### 3.11. GA Down-Regulates the Melanogenic Genes in UVB-Irradiated B6 Mouse Skin

The inhibitory effects of GA on melanogenic regulatory proteins, including tyrosinase and MITF, were apparent in cultured B16F10 melanoma cells. To delineate this phenomenon *in vivo*, the protein expression levels of tyrosinase and MITF were examined by immunohistochemistry using monoclonal anti-tyrosinase and MITF antibodies. The results showed that GA treatment led to a significant decrease in tyrosinase and MITF expression when compared with control or UVB-irradiated groups (Figs. 6D and 6E). More precisely, UVB irradiation

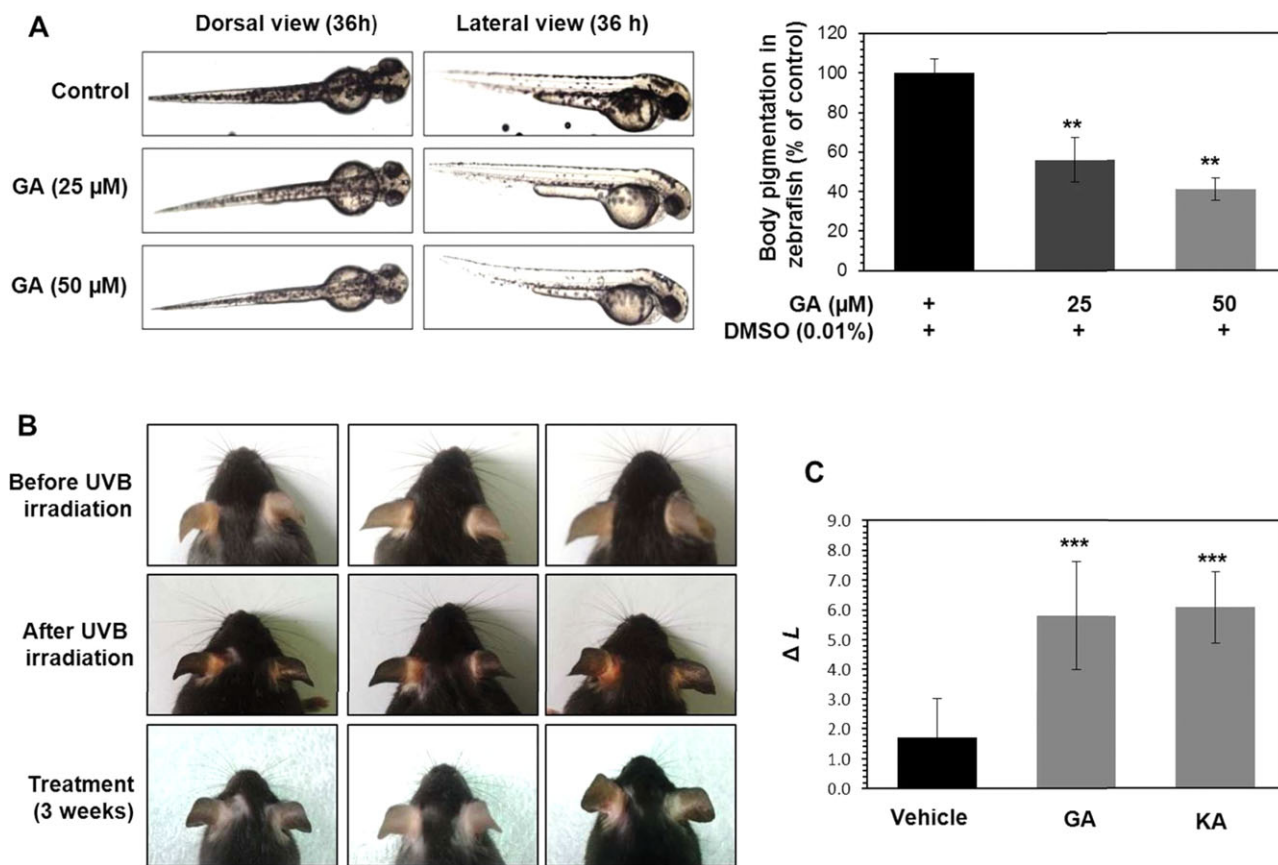


**FIG 5**

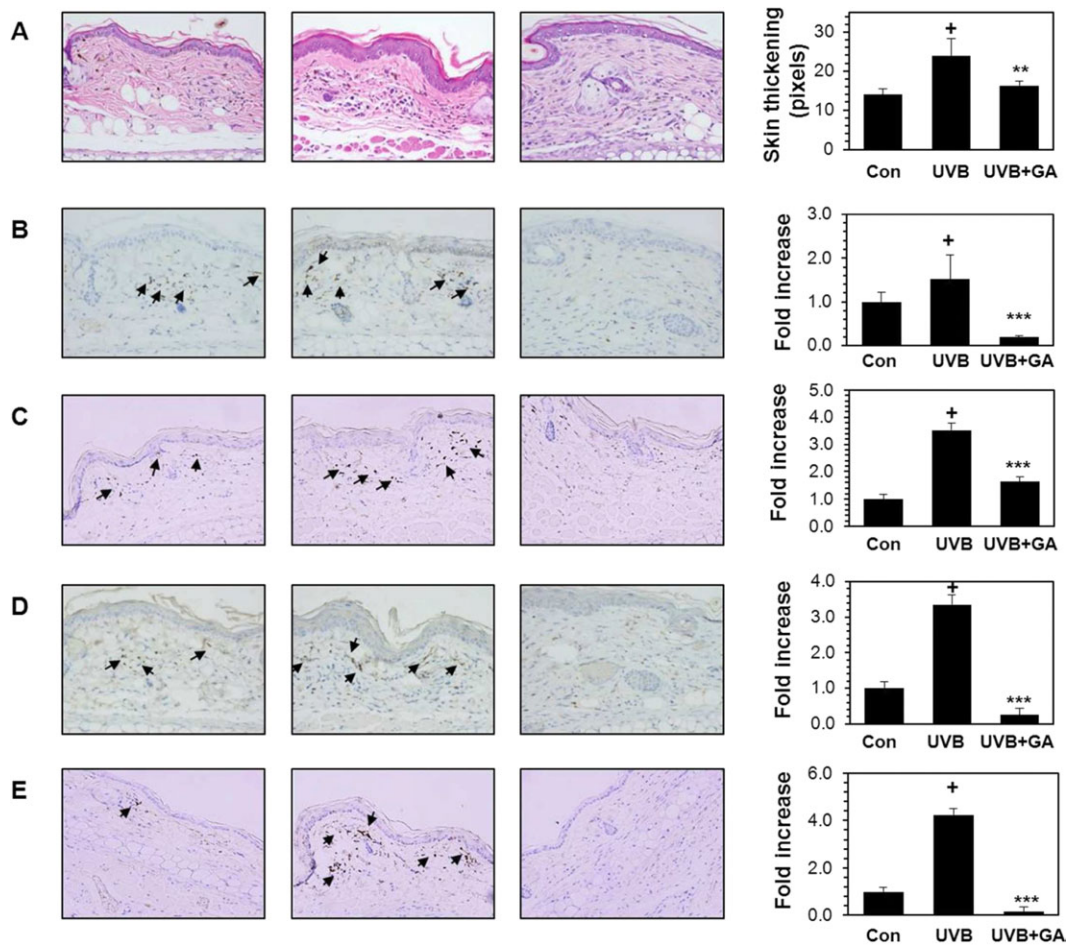
The effects GA on melanogenesis in zebrafish and skin lightening in UVB-induced B6 mice. (A) 24 H post-fertilized embryos were incubated with GA for 36 H. The effects of endogenous body pigmentation of zebrafish were observed using a stereomicroscope. The dorsal and lateral views were shown. The body pigmentation was quantified by Image pro-plus software pack. (B) Representative photographs showing the skin lightening effect of GA on UVB-induced hyperpigmentation. Normal skin color (before UV-irradiation) is shown in the upper panels, UVB-induced hyperpigmented skin is shown in middle panels and the lower panels show the lightening effects of GA after topical application for 3 weeks. KA was used as a drug control. (C) The degree of pigmentation ( $\Delta L$ -value) before and after 4 weeks of GA application. The results are presented as the mean  $\pm$  SD of three independent experiments. Statistical significance \* $P < 0.05$ , \*\* $P < 0.01$ , and \*\*\* $P < 0.001$  were defined as control versus sample.

induced 3.3-fold and 4.2-fold increases in tyrosinase and MITF protein expression, respectively. The topical application of GA resulted in 0.25-fold and 0.17-fold decreases in tyrosinase and MITF protein levels, respectively (Figs. 6D and 6E). These results provide *in vivo* evidence that the GA-mediated depigmenting effect results from the down-regulation of the melanogenic regulatory genes.

## 4. Discussion

The use of tyrosinase inhibitors is becoming increasingly important in the cosmetic and pharmaceutical industries due to their skin whitening and protective effects. A large number of tyrosinase inhibitors derived from natural sources have already been reported. Arbutin, kojic acid, and ascorbic acid are

examples of tyrosinase inhibitors currently in use [2]. GA and its derivatives are widely used as food additives and are rich in green tea and Chinese toon [19,20]. Kim et al [10] initially characterized the inhibitory effects of GA against mushroom tyrosinase activity and showed that the 50% inhibition concentration for mushroom tyrosinase activity was 3.5  $\mu\text{M}$ , which is less than that of the commercial tyrosinase inhibitor KA ( $\text{IC}_{50} = 59.7 \mu\text{M}$ ). It is known that tyrosinase has both monophenolase and diphenolase activity that can catalyze the hydroxylation of a monophenol and the conversion of *O*-diphenol to the corresponding *O*-quinone [21]. In the present study, we used *L*-tyrosine as a substrate to determine the monophenolase activity and *L*-DOPA to test the diphenolase activity. We determined that the concentrations for GA required for 50% inhibition of mushroom tyrosinase activity are 25.69  $\mu\text{M}$  for monophenolase and 61.63  $\mu\text{M}$  for diphenolase activity (Tables 2


**FIG 6**

The effects of GA on UVB-induced hyperpigmentation in B6 mice. (A) Histological analysis of ear skin samples from B6 mice. Biopsy specimens from the GA-treated and control sites after 4 weeks of GA application were processed for light microscopy examination by H&E staining. In control mice, slight (2) melanocyte aggregation with melanin pigment was found in the subcutis of the ear. In UVB-irradiated mice, moderate/severe (4) melanocyte aggregation with melanin pigment and inflammatory cell infiltration (arrow) were found in the subcutis of ear. In GA-treated mice, slight (2) melanocyte aggregation with melanin pigment was found in the subcutis of ear. (B–D) Immunohistochemistry of B6 mice ear skin samples with L-DOPA (B), melanosome GP100 (C), tyrosinase (D), and MITF (E) antibodies. The relative intensity of antibody positive staining cells was quantified by Image pro-plus software. The results are presented as the mean  $\pm$  SD of three independent experiments. Statistical significance  $^{*}P < 0.01$  was defined as control versus sample.

and 3). However, our data are somewhat contrasting to the previous observations by Kim et al [10], which showed the IC<sub>50</sub> value of GA against mushroom tyrosinase was 3.5  $\mu$ M. That value is nearly 7-fold lower than our value (25.69  $\mu$ M). GA has been reported to strongly inhibit murine tyrosinase activity in cultured melanoma cells, and the reduction in melanin synthesis is known to be associated with the inhibition of tyrosinase activity [5,14]. The results of the present study also show that tyrosinase and tyrosinase-related proteins, including TRP-1 and Dct, are down-regulated by GA at both the transcriptional and translational levels.

MITF is a transcription factor that binds to the M/E-box of tyrosinase, TRP-1, and Dct promoters and initiates the transcription of genes required for melanin biosynthesis [4]. Therefore, we monitored MITF expression in response to GA treat-

ment. Our results showed that GA caused a marked reduction in MITF expression and nuclear translocation. A similar result was also observed from an MITF knock-down with siRNAs. Several upstream kinases have been found to phosphorylate MITF at specific serine residues, including Ser73, Ser298, and Ser409, which leads to its ubiquitin-mediated proteasomal degradation. In particular, ERK activation by small molecules in murine melanoma or human melanocytes inhibits melanin biosynthesis through the proteasomal degradation of MITF by the phosphorylation at Ser73 [22]. Additionally, it has been demonstrated that the pharmacological inhibition of ERK by a specific inhibitor increased melanin biosynthesis [10]. In our study, we found that GA-induced ERK phosphorylation, reduced melanin synthesis and down-regulated MITF expression. Previous studies have also shown that the activation of

TABLE 2

**Mushroom tyrosinase inhibitory effects of test compounds. Mushroom tyrosinase (21,000 U/mL) was incubated with the indicated concentrations of test compounds for 10 Min at room temperature prior to incubation with 1.5 mM of L-tyrosine for 30 Min**

Sample	IC <sub>50</sub> , $\mu$ M	Mushroom tyrosinase activity (monophenolase)				
		0 $\mu$ M	12.5 $\mu$ M	25 $\mu$ M	50 $\mu$ M	100 $\mu$ M
Gallic acid	25.69	100	77.8	57.4	26.4	5.5
Kojic acid	14.34	100	58.2	39.5	16.4	4.8
Arbutin	128.1	100	71.5	67.4	63.3	69.0
Quercetin	126.1	100	70.3	68.2	62.8	58.2
Ascorbic acid	14.57	100	50.3	50.2	25.9	5.5

The absorbance was determined at 490 nm. Each value represents the mean of three independent experiments.

Akt/PKB suppressed melanin production in human melanoma G631 and murine melanocyte Melan-A cells [10,23]. Inhibition of the Akt pathway by the Akt inhibitor LY294002 increased melanin synthesis in B16 melanoma cells [24]. Our data showed that GA increased phosphorylation of Akt, inhibited melanin synthesis and led to the down-regulation of MITF. Conversely, treatment with LY294002 increased melanin production in melanoma cells. Taken together, our findings are in agreement with other observations that natural compound-induced ERK/Akt activation might be involved in melanogenesis [10,22,25].

MC1-R is a transmembrane receptor expressed in melanocytes and melanoma cells that is activated by  $\alpha$ -MSH and increases intracellular cAMP. PKA has been reported to be involved in cAMP-induced melanogenesis through the activation of CREB phosphorylation, which consequently transcribes MITF [26]. In this study, the phosphorylation of CREB

was inhibited by GA. To confirm our findings, we investigated the upstream kinases of CREB, PKA, and cAMP. Treatment with GA led to a sustained reduction in PKA and cAMP expression in  $\alpha$ -MSH-induced melanoma cells. These data strengthen the possibility that GA-induced inhibition of melanin synthesis occurs through the transcriptional inhibition of CREB.

Recently, Panich et al [27] reported that UVA-induced proliferation and melanogenesis in melanoma cells was inhibited by GA through mimicking their anti-oxidative properties. Several *in vivo* studies using murine or human models also demonstrated that the topical or oral administration of phytochemicals or herbal extracts reduced the incidence of UV-induced hyperpigmentation [6,8,9,18]. In our study, we observed efficient skin lightening effects in response to topical GA application to the UVB-irradiated B6 mouse ear skin. Immunohistochemical analyses revealed that the de-pigmenting effect of GA on UVB-induced B6 mice is possibly caused by the

TABLE 3

**Mushroom tyrosinase inhibitory effects of test compounds. Mushroom tyrosinase (21,000 U/mL) was incubated with the indicated concentrations of test compounds for 10 Min at room temperature prior to incubation with 15 mM of L-DOPA for 30 Min**

Sample	IC <sub>50</sub> , $\mu$ M	Mushroom tyrosinase activity (diphenolase)				
		0 $\mu$ M	12.5 $\mu$ M	25 $\mu$ M	50 $\mu$ M	100 $\mu$ M
Gallic acid	61.63	100	86.8	74.7	41.8	25.2
Kojic acid	18.04	100	53.9	45.0	26.4	16.2
Arbutin	5.23	100	24.5	18.9	15.2	10.5
Quercetin	72.72	100	82.9	68.3	58.0	30.1
Ascorbic acid	26.93	100	76.4	62.3	19.1	5.3

The absorbance was determined at 475 nm. Each value represents the mean of three independent experiments.



down-regulation of melanogenic markers, including tyrosinase and MITF. In addition, we investigated the phenotype-based skin whitening effect of GA using a zebrafish model. The treatment of 24 h post-fertilized zebrafish embryos with GA for 36 h showed a marked reduction in body pigmentation.

In summary, previous studies successfully characterized GA as a potent tyrosinase inhibitor. In this article, we demonstrated that GA exerts hypopigmentary effects through inhibition of melanogenic regulatory genes, including tyrosinase, TRP-1, Dct, and MITF, *in vitro* and that its effects are further regulated by the down-regulation of cAMP pathway. However, the primary target of GA is blocking MCR-1 receptor system, which eventually inhibits their downstream cascades including activation of cAMP/PKA/CREB and MITF. In addition, GA also significantly induced the protective mechanism by activating the ERK and AKT kinases, which induce proteasomal degradation of MITF. Our results obtained from *in vivo* experiments showed that GA potentially ameliorates and reverses the UVB-induced hyperpigmentation and zebrafish body pigmentation. These findings imply that GA can be developed as a skin lightening or therapeutic agent for hyperpigmentary skin diseases.

## CONFLICT OF INTEREST

The authors state no conflicts of interest.

## Acknowledgements

This work was supported by grants NSC-99-2320-B-039-035-MY3, NSC-98-2320-B-039-037-MY3, and CMU 98-C09 from the National Science Council and China Medical University, Taiwan.

## References

- [1] Shin, Y. J., Han, C. S., Lee, C. S., Kim, H. S., Ko, S. H., et al. (2010) Zeolite 4A, a synthetic silicate, suppresses melanogenesis through the degradation of microphthalmia-associated transcription factor by extracellular signal-regulated kinase activation in B16F10 melanoma cells. *Biol. Pharm. Bull.* 33, 72–76.
- [2] Kim, Y. J., and Uyama, H. (2005) Tyrosinase inhibitors from natural and synthetic sources: structure, inhibition mechanism and perspective for the future. *Cell. Mol. Life Sci.* 62, 1707–1723.
- [3] Yoon, W. J., Kim, M. J., Moon, J. Y., Kang, H. J., Kim, G. O., et al. (2010) Effect of palmitoleic acid on melanogenic protein expression in murine b16 melanoma. *J. Oleo. Sci.* 59, 315–319.
- [4] Park, H. Y., Kosmadaki, M., Yaar, M., and Gilcherst, B. A. (2009) Cellular mechanisms regulating human melanogenesis. *Cell. Mol. Life Sci.* 66, 1493–1506.
- [5] Sato, K., and Toriyama, M. (2005) Effect of pyrroloquinoline quinone (PQQ) on melanogenic protein expression in murine B16 melanoma. *J. Dermatol. Sci.* 53, 140–145.
- [6] Park, K. T., Kim, J. K., Hwang, D., Yoo, Y., and Lim, Y. H. (2011) Inhibitory effect of mulberroside A and its derivatives on melanogenesis induced by ultraviolet B irradiation. *Food Chem. Toxicol.* 49, 3038–3045.
- [7] Choi, S., Lee, S. K., Kim, J. E., Chung, M. H., and Park, Y. I. (2002) Aloesin inhibits hyperpigmentation induced by UV radiation. *Clin. Exp. Dermatol.* 27, 513–515.
- [8] Yamakoshi, J., Otsuka, F., Sano, A., Tokutake, S., Saito, M., et al. (2003) Lightening effect on ultraviolet-induced pigmentation of guinea pig skin by oral administration of a proanthocyanidin-rich extract from grape seeds. *Pigment Cell Res.* 16, 629–638.
- [9] Yoshimura, M., Watanabe, Y., Kasai, K., Yamakoshi, J., and Koga, T. (2005) Inhibitory effect of an ellagic acid-rich pomegranate extract on tyrosinase activity and ultraviolet-induced pigmentation. *Biosci. Biotechnol. Biochem.* 69, 2368–2373.
- [10] Kim, J. H., Baek, S. H., Kim, D. H., Choi, T. Y., Yoon, T. J., et al. (2007) Downregulation of melanin synthesis by haginin A and its application to *in vivo* lightening model. *J. Invest. Dermatol.* 128, 1227–1235.
- [11] Kumar, K. J. S., Yang, J. C., Chu, F. H., Chang, S. T., and Wang, S. Y. (2010) Lucidone, a novel melanin inhibitor from the fruit of *Lindera erythrocarpa* Makino. *Phytother. Res.* 24, 1158–1165.
- [12] Lv, N., Koo, J. H., Yoon, H. Y., Yu, J., Kim, K. A., et al. (2007) Effect of *Angelica gigas* extract on melanogenesis in B16 melanoma cells. *Int. J. Mol. Med.* 20, 763–767.
- [13] Cui, R., Widlund, H. R., Feige, E., Lin, J. Y., Wilensky, D. L., et al. (2007) Central role of p53 in the suntan response and pathologic hyperpigmentation. *Cell* 128, 853–864.
- [14] Kim, Y. J. (2007) Antimelanogenic and antioxidant properties of gallic acid. *Biol. Pharm. Bull.* 30, 1052–1055.
- [15] Sekulic, A., Haluska, P. Jr., Miller, A. J., Genebriera De Lamo, J., Ejadi, S., et al. (2008) Malignant melanoma in the 21st century: the emerging molecular landscape. *Mayo Clin. Proc.* 83, 825–846.
- [16] Khaled, M., Larribere, L., Bille, K., Aberdam, E., Ortonne, J. P., et al. (2002) Glycogen synthase kinase 3beta is activated by cAMP and plays an active role in the regulation of melanogenesis. *J. Biol. Chem.* 277, 33690–33697.
- [17] Ebanks, J. P., Wickett, R. R., and Boissy, R. E. (2009) Mechanisms regulating skin pigmentation: the rise and fall of complexion coloration. *Int. J. Mol. Sci.* 10, 4066–4087.
- [18] Leyden, J. J., Shergill, B., Micali, G., Downie, J., and Wallo, W. (2011) Natural options for the management of hyperpigmentation. *J. Eur. Acad. Dermatol. Venereol.* 25, 1140–1145.
- [19] Cabrera, C., Gimenez, R., and Lopez, M. C. (2003) Determination of tea components with antioxidant activity. *J. Agric. Food Chem.* 51, 4427–4435.
- [20] Chia, Y. C., Rajbanshi, R., Calhoun, C., and Chiu, R. H. (2010) Anti-neoplastic effects of gallic acid, a major component of *Toona sinensis* leaf extract, on oral squamous carcinoma cells. *Molecules* 15, 8377–8389.
- [21] Lin, Y. F., Hu, Y. H., Jia, Y. L., Li, Z. C., Guo, Y. J., et al. (2012) Inhibitory effects of naphthols on the activity of mushroom tyrosinase. *Int. J. Biol. Macromol.* doi: 0.1016/j.ijbiomac.2012.04.026.
- [22] Choi, Y. G., Bae, E. J., Kim, D. S., Park, S. H., Kwon, S. B., et al. (2006) Differential regulation of melanosomal proteins after hinokitiol treatment. *J. Dermatol. Sci.* 43, 181–188.
- [23] Oka, M., Nagai, H., Ando, H., Fukunaga, M., Matsumura, M., et al. (2000) Regulation of melanogenesis through phosphatidylinositol 3-kinase-Akt pathway in human G361 melanoma cells. *J. Invest. Dermatol.* 115, 699–703.
- [24] Busca, R., Bertolotto, C., Ortonne, J. P., and Ballotti, R. (1996) Inhibition of the phosphatidylinositol 3-kinase/p70(S6)-kinase pathway induces B16 melanoma cell differentiation. *J. Biol. Chem.* 271, 31824–31830.
- [25] Smit, N., Vicanova, J., and Pavel, S. (2009) The hunt for natural skin whitening agents. *Int. J. Mol. Sci.* 10, 5326–5349.
- [26] Wan, P., Hu, Y., and He, L. (2011) Regulation of melanocyte pivotal transcription factor MITF by some other transcription factors. *Mol. Cell Biochem.* 354, 241–246.
- [27] Panich, U., Onkokoong, T., Limsaengurai, S., Akaraseenont, P., and Wongkajornsilp, A. (2012) UVA-induced melanogenesis and modulation of glutathione redox system in different melanoma cell lines: the protective effect of gallic acid. *J. Photochem. Photobiol. B* 108, 16–22.